Approximate Closed-Form Formula for Calculating Ohmic Resistance in Coils of Parallel Round Wires With Unequal Pitches

Jinwook Kim, *Member, IEEE*, and Young-Jin Park, *Member, IEEE*

***Abstract*—An approximate closed-form formula for calculating the ohmic resistance of a circular multiloop coil with unequal pitches is presented. Skin effect and proximity effect are included in the formula. The proximity effect is expressed as a proximity factor obtained using transverse magnetic fields applied to a wire from the rest of the wires. For verification, the optimum dimension for minimum resistance of wires with an equal pitch is compared with the previous results, and both results agree. The formula is applied to calculate the ohmic resistance of helical and spiral coils and is verified by a 2-D finite-element-method simulation. Both calculation and simulation results are consistent as well. As a practical application, a spiral coil with unequal pitches is designed for uniform mutual inductance, and it is optimized for the lowest resistance using the formula. The measured ohmic resistance of the designed coil also agrees with the calculated and simulated results. The results show that the formula can be well applied to designing circular multiloop coils with minimum ohmic loss in wireless-power-transfer systems.**

***Index Terms*—Multiloop coil, ohmic resistance, parallel round wires, proximity effect, skin effect, wireless power transfer (WPT).**

I. Introduction

MULTILOOP coils with equal pitch, such as conventional helical [1]–[5] and spiral coils [6]–[9], have been widely used for generating strong magnetic fields in magnetic resonance wireless power transfer (WPT) systems. Recently, multiloop coils with unequal pitches have been also currently employed for free positioning in magnetic resonance WPT systems because the coils of these windings can generate uniform magnetic field (H-field) distribution with respect to the horizontal movement of a receiving (Rx) coil [10], [11].

Ohmic losses of coils in magnetic resonance WPT systems are the main cause of efficiency degradation. Hence, it is necessary to reduce the ohmic loss of the multiloop coils. In [5], [10], and [11], coils were made by a litz wire to reduce ohmic loss because hundreds of kilohertz of frequencies for WPT were used. However, recently, many applications of magnetic resonance WPT are made at a frequency higher than several megahertz [1]–[4], [6]–[9]. At a high frequency, solid or tubular conductor wires are used to produce lower ohmic loss instead of litz wires because resistance to skin effects as well as proximity effects rises considerably at a frequency higher than several megahertz.

Several methods have been reported for calculating the ohmic resistance of multiloop coils, with a solid wire considering both skin and proximity effects. In [12]–[15], multiloop coils with an equal pitch only were considered. In [16], a resistance calculation method by using a 3-D finite-difference time domain was proposed for helical coils with arbitrary windings. However, the computation time increases with the number of turns, and the optimum process for achieving the lowest ohmic loss of coils was not also shown.

In this paper, a simple approximate closed-form formula of ohmic resistance for circular multiloop coils with both equal and unequal pitches of solid round wires is proposed. The formula consists of resistance by skin and proximity effects. The calculation results are verified with previous works and 2-D finite-element method (FEM) simulation results as well. It is also shown that the ohmic resistance of multiloop coils with unequal pitches can be minimized using the derived formula.

II. Resistance by Skin and Proximity Effects

To derive the ohmic resistance of a circular multiloop coil with unequal pitches, the following assumptions are made: Solid round wires are identical, identical currents in the wires flow in the same direction, and there is no current variation along longitudinal directions in the wire.

Fig. 1(a) shows the current density distribution on a cross section of an isolated solid round wire without an H-field. The net current and radius of the wire are represented as I_0 and r_0, respectively. The color bar shows the current density $(\mathrm{A/m^2})$. Because of the skin effects that occur under high frequencies, the current is confined to the surface of the wire, and there is no current in the middle of the wire. It is observed that the current density is rotationally symmetric. With a sufficiently high operating frequency and the radius of the wire, r_0, being larger than the skin depth, $\delta = 1/(\pi f \mu_0 \sigma)^{1/2}$ $(r_0/\delta > 1)$, the

Manuscript received March 14, 2014; revised March 17, 2014 and June 14, 2014; accepted October 22, 2014. Date of publication November 20, 2014; date of current version May 8, 2015. *(Corresponding author: Young-Jin Park.)*

J. Kim was with the University of Science and Technology, Ansan 426-910, Korea. He is now with the Korea Electrotechnology Research Institute (KERI), Ansan 426-910, Korea (e-mail: jwkim@ust.ac.kr).

Y.-J. Park is with the University of Science and Technology, Ansan 426-910, Korea, and also with the Korea Electrotechnology Research Institute, Ansan 426-910, Korea (e-mail:yjpark@keri.re.kr).

Color versions of one or more of the figures in this paper are available online at http://ieeexplore.ieee.org.

Digital Object Identifier 10.1109/TIE.2014.2370943

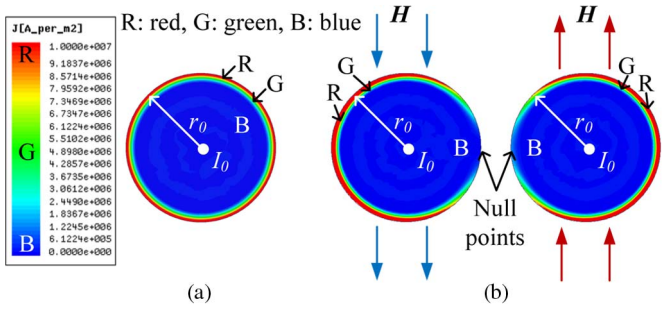

Fig. 1. Current density distribution on a cross section of a wire, where (a) represents the isolated solid round wire and (b) represents the two neighboring wires.

asymptotic representation of resistance per unit length due to skin effects is given as follows [17]:

$$R_{skin} = R_{DC}\left(\frac{1}{4} + \frac{r_0}{2\delta} + \frac{3}{32}\frac{\delta}{r_0}\right) \ (\Omega/\text{m}). \tag{1}$$

$R_{DC} = 1/(\pi r_0^2 \sigma)$, where σ is the conductivity of the wire, f is an operating frequency, and μ_0 is the permeability in vacuum.

Fig. 1(b) shows two neighboring wires. Each wire has the identical net current I_0. H-fields generated by one wire are applied to another wire, and they influence the current distribution in each wire. Equivalent currents induced by the applied H-field are made on the surface of the wire, and the current distribution is no longer rotationally symmetric due to the proximity effect. The resistance (R_{prox}) by the proximity effect in Fig. 1(b) can be expressed as follows [17]:

$$R_{prox} = \frac{2P_{prox}}{I_0^2} \approx 2R_{DC}\pi^2 r_0^2\left(\frac{2r_0}{\delta} - 1\right)\frac{H^2}{I_0^2}(\Omega/\text{m}). \tag{2}$$

Here, P_{prox} is the power loss due to the proximity effect. From (2), it is found that R_{prox}, at an operating frequency, is determined mainly by the applied H-field (H) when the r_0, $\mu 0$, and σ of the wire are given.

To evaluate the loss by the proximity effect according to that by the skin effect, the ratio of R_{prox} to R_{skin}, called a proximity factor (G_p), is defined as follows:

$$G_p = \frac{R_{prox}}{R_{skin}} = \frac{2\pi^2 r_0^2\left(\frac{2r_0}{\delta} - 1\right)H^2}{\left(\frac{1}{4} + \frac{r_0}{2\delta} + \frac{3}{32}\frac{\delta}{r_0}\right)I_0^2} = \frac{8\pi^2\delta^2 x^3(x-1)}{(2x+1)^2+2}\frac{H^2}{I_0^2} \tag{3}$$

where $x = 2r_0/\delta = d/\delta$. As a result, the ohmic resistance (R_{ohmic}) per unit length of the wire is expressed as follows using the proximity factor:

$$R_{\text{ohmic}} = R_{skin} + R_{prox} = R_{skin}(1 + G_p) \quad (\Omega/\text{m}). \tag{4}$$

It is true that skin and proximity effects can be divided by their orthogonality [14], [15]. Therefore, it should be noted that, to obtain the ohmic resistance of multiloop coils (R_{ohmic}) per unit length, the resistance by the proximity effect (R_{prox}) can be achieved by substituting the summation of H-fields applied to every wire from the other wires into (2), while the resistance by the skin effect (R_{skin}) can be obtained from (1). The total ohmic resistance can be calculated by multiplying R_{ohmic} by the length of the total wire.

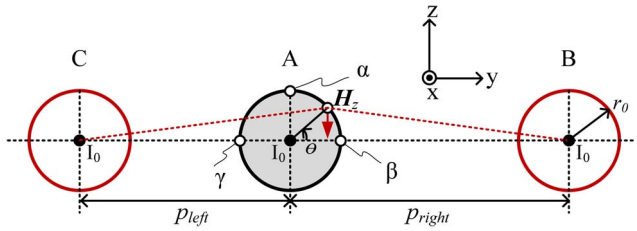

Fig. 2. Schematic diagram for the calculation of z-directed H-fields applied to target wire A by source wires B and C.

III. Proximity Effects Among Parallel Round Wires

A. Calculation of H-Fields Applied From Other Wires

For the calculation of a proximity-effect loss, an entire H- field applied to every wire from the other wires is required as explained in the previous section. For these purposes, at first, H-fields applied to a wire from the other wires are calculated, and an equivalent total H-field is derived by adding all H-fields obtained from each wire.

Fig. 2 shows a schematic diagram for calculating z-directed H-fields on the surface of a target wire A by left- and right-side wires (B and C). Both p and θ denote the gap between the wires and an angle on the surface, respectively. For the calculation, it is assumed that the current source wires (B and C) are filamentary. The net current of each wire is I_0. Since the current is confined near the surface at a high frequency, the z-directed H-field intensities from right- and left-side wires are, according to the angle θ, as follows, respectively,

$$\boldsymbol{H}_{z,right} = -\hat{z}\frac{I_0}{2\pi}\cdot\frac{p_{right} - r_0\cos\theta}{p_{right}^2 + r_0^2 - 2p_{right}r_0\cos\theta} \tag{5-1}$$

$$\boldsymbol{H}_{z,left} = \hat{z}\frac{I_0}{2\pi}\cdot\frac{p_{left} + r_0\cos\theta}{p_{left}^2 + r_0^2 + 2p_{left}r_0\cos\theta}. \tag{5-2}$$

Three reference points α, β, and γ are chosen for the calculation of an equivalent H-field applied to the target wire A. The reference point α is at $\theta = 90°$, whereas the reference points β and γ are at $\theta = 0°$ and $\theta = 180°$, respectively. The reference point α is a middle point of a surface of a wire cross section.

The reference points β and γ are the most affected points by adjacent right- and left-side wires, respectively. Therefore, the magnitudes of H-fields at each reference point are as follows:

$$H_{\alpha,left} = \frac{I_0}{2\pi}\cdot\frac{p_{left}}{p_{left}^2 + r_0^2} \tag{6-1}$$

$$H_{\alpha,right} = \frac{I_0}{2\pi}\cdot\frac{p_{right}}{p_{right}^2 + r_0^2} \tag{6-2}$$

$$H_\beta = H_{\beta,left} - H_{\beta,right} = \frac{I_0}{2\pi}\left(\frac{1}{p_{left} + r_0} - \frac{1}{p_{right} - r_0}\right) \tag{6-3}$$

$$H_\gamma = H_{\gamma,left} - H_{\gamma,right} = \frac{I_0}{2\pi}\left(\frac{1}{p_{left} - r_0} - \frac{1}{p_{right} + r_0}\right). \tag{6-4}$$

Fig. 3 shows the configuration for the calculation of H-fields applied to the mth wire (target wire) from the other wires in N

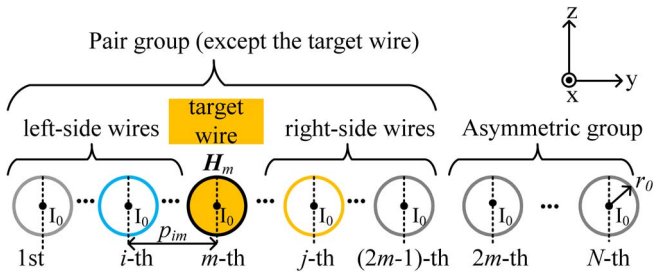

Fig. 3. Configuration in calculating H-fields when applied to the mth wire in a system of N parallel wires.

parallel wires. To calculate the H-fields applied to the target wire from other wires, they, except for the target wire, are divided into two groups according to their positions based on the target wire as follows.

1) Pair group: Wires in the group where a left-side wire corresponds to a right-side wire based on the target wire.
2) Asymmetric group: Wires in the group where a left-side wire corresponds to a right-side wire do not exist and vice versa.

When source wires belong to the pair group, H-fields from both a left-side wire and its corresponding right-side wire are calculated simultaneously at the reference points β and γ, respectively. Because a proximity power loss is proportional to the square of H-fields from (2), the equivalent H-field applied to a target wire ($\boldsymbol{H}_{\text{pair}}$) from a pair of wires is obtained by the power mean as follows:

$$\boldsymbol{H}_{\text{pair}} = \hat{z}\sqrt{\frac{1}{2}\left(H_\beta^2 + H_\gamma^2\right)} \tag{7}$$

where H_β and H_γ denote the scalar H-fields from left- and right-side wires at the reference points β and γ, respectively. When source wires belong to the asymmetric group, the H-fields applied to the target wire are calculated at the reference point α from (5-1) or (5-2).

By applying the equivalent H-fields from (6) and (7) to N parallel wires with unequal pitches, all H-fields at each wire can be obtained. Therefore, the H-field applied to the mth wire from the ith and jth pair wires is calculated from (8), shown at the bottom of the page, where $i + j = 2m$. The total H-field applied to the mth wire from wires in a pair group, $H_{m,\text{pair}}$, is calculated according to m as follows:

$$\mathrm{H}_{m,\text{pair}} = \begin{cases} 0, & \text{for } m = 1 \text{ and } N \\ \sum_{i=1}^{m-1} \mathrm{H}_{m,\text{pair}}(i,j), & \text{for } 1 < m \le \lceil N/2 \rceil \\ \sum_{i=2m-N}^{m-1} \mathrm{H}_{m,\text{pair}}(i,j), & \text{for } \lceil N/2 \rceil < m < N. \end{cases} \tag{9}$$

Now, the H-field applied to the mth wire from the kth asymmetric wire is obtained at point α as follows:

$$\boldsymbol{H}_{m,\text{asy}}(k) = \hat{z}H_{m,\text{asy}}(k) = -\hat{z}\frac{I_0}{2\pi} \cdot \frac{p_{mk}}{p_{mk}^2 + r_0^2}. \tag{10}$$

Thus, the total H-field applied to the mth wire from the wires in an asymmetric group, $H_{m,\text{asy}}$, is calculated according to m as follows:

$$H_{m,\text{asy}} = \begin{cases} 0, & \text{for } m = N/2 \\ \sum_{k=2m}^{N} H_{m,\text{asy}}(k), & \text{for } 1 \le m \le \lceil N/2 \rceil \\ \sum_{k=1}^{2m-N-1} H_{m,\text{asy}}(k), & \text{for } \lceil N/2 \rceil < m < N \\ \sum_{k=1}^{N-1} H_{m,\text{asy}}(k), & \text{for } m = N. \end{cases} \tag{11}$$

By adding both $\boldsymbol{H}_{m,\text{pair}}$ and $\boldsymbol{H}_{m,\text{asy}}$, the equivalent total H-field applied to the mth wire from the other wires $\boldsymbol{H}_m$ can be expressed as follows:

$$\boldsymbol{H}_m = \boldsymbol{H}_{m,\text{pair}} + \boldsymbol{H}_{m,\text{asy}} = \hat{\boldsymbol{z}}H_m. \tag{12}$$

B. Proximity Factor G_p and Ohmic Resistance

The proximity factor in a system of N parallel wires depends on the number of wires. Therefore, by substituting (12) into (3), the proximity factor G_p for N parallel solid round conductor wires can be obtained as follows:

$$G_p = \frac{8\pi^2\delta^2x^3(x-1)}{(2x+1)^2+2}\left(\frac{1}{N}\sum_{m=1}^{N}\frac{H_m^2}{I_0^2}\right). \tag{13}$$

Then, the total ohmic resistance per unit length is achieved by substituting (1) and (13) into (4) as follows:

$$R_{\text{ohmic}} = \frac{R_{DC}}{16x} \times \left[(2x+1)^2 + 2 + \frac{8\pi^2\delta^2x^3(x-1)}{N}\left(\sum_{m=1}^{N}\frac{H_m^2}{I_0^2}\right)\right]. \tag{14}$$

It is noted that the ohmic resistance per unit length in a system of N parallel round wires with unequal pitches is derived as a closed-form formula. The results can also be applied to the calculation of the ohmic resistance in a multiloop conductor coil with circular cross sections and equal or unequal pitches.

$$\begin{aligned} \boldsymbol{H}_{m,\text{pair}}(i,j) &= \hat{z}H_{m,\text{pair}}(i,j) \\ &= -\hat{z}\frac{I_0}{2\pi}\sqrt{\frac{p_{im}^2+r_0^2}{\left(p_{im}^2-r_0^2\right)^2} + \frac{p_{mj}^2+r_0^2}{\left(p_{mj}^2-r_0^2\right)^2} - \frac{2\left(p_{im}p_{mj}-r_0^2\right)}{\left(p_{im}^2-r_0^2\right)\left(p_{mj}^2-r_0^2\right)}} \end{aligned} \tag{8}$$

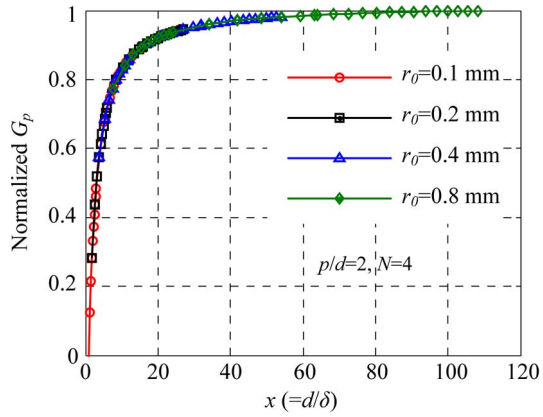

Fig. 4. Normalized G_p for parallel round wires with an equal pitch when $N = 4$, $p/d = 2$, and the wire radius r_0 is from 0.1 to 0.8 mm.

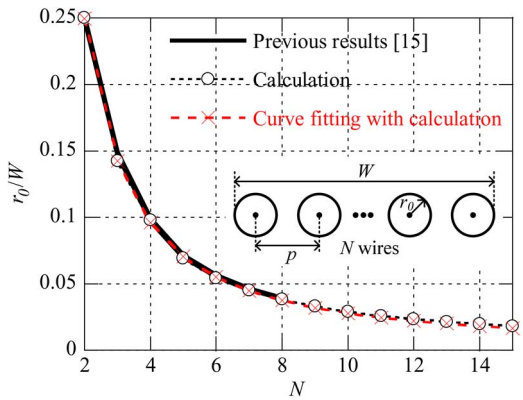

Fig. 5. Representation of the optimum conditions of r_0/W, for minimum resistance (OMR) as a function of N.

IV. Calculation of Optimum Conditions for Minimum Ohmic Resistance of N Parallel Wires

A. Normalized Proximity Factor G_p

The proximity factor derived in (15) is a function of x, N, and H, where x includes the skin depth δ and wire diameter d. Fig. 4 shows the calculation results of G_p normalized by the maximum value, depending on x. The normalized G_p did not change irrespective of pitches and the number of turns since the normalized G_p is a function of not N or H, but x only. The normalized G_p increases as x increases. As a result, the proximity factor in (13) is frequency dependent, and its dominant factors are the wire diameter and operating frequency. Hence, the proximity-effect loss can be minimized by choosing an optimum wire diameter at a fixed frequency.

B. Optimum Conditions for Minimum Resistance (OMR) in N Parallel Wires With an Equal Pitch

Fig. 5 shows the calculated optimum value of r_0/W for minimum resistance (OMR) according to a function of N and the previous results in [15] for comparison. The winding width of parallel wires is denoted as W. The solid line and circular dotted line represent the previous results and the calculation, respectively. It is observed that the maximum difference between the calculated results of OMR and the previous results for $N = 2, 3, \ldots, 8$ is 3.85%. This conclusion shows that both results are in excellent agreement.

From a practical viewpoint, a useful formula for OMR can be derived by using a curve-fit method with the power law based on the calculation results as follows:

$$OMR = \frac{r_0}{W} = 0.6534N^{(-1.397)} + 0.001815,\ N = 2, 3, \ldots. \tag{15}$$

In Fig. 5, the $\times$-marked dotted line represents the results calculated using (15) for $N = 2, 3, \ldots, 15$. It can be observed that the results using the formula for OMR are in agreement with those in [15]. It should be pointed out that the OMR in (15) can be effectively applied to find the optimal value of the radius when W and N are given.

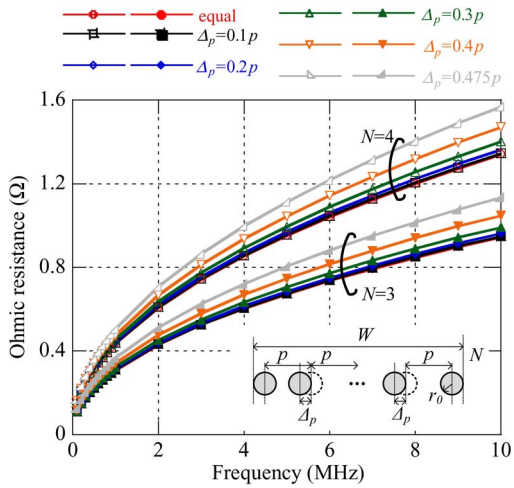

Fig. 6. Calculated ohmic resistances for N parallel wires as a function of pitches, when $r_0 = 0.5$ mm, $p = 2$ mm, and $N = 3$ and 4. The length of each wire is 1 m.

C. Ohmic Resistance of N Parallel Wires According to Variation of Pitches

Fig. 6 shows the calculated ohmic resistances of N parallel wires, according to pitches when $r_0 = 0.5$ mm and $p = 2$ mm. Two cases of $N = 3$ and 4 are considered. The length of each wire is determined to be 1 m. With W and r_0 fixed, pitches decrease as much as the variation of pitches Δ_p from 0.1p to 0.475p. It is found that minimum resistance is achieved when the pitches are equal $(\Delta_p = 0)$ in both $N = 3$ and 4. Ohmic resistances are almost the same until the variation of pitches is 20%. On the contrary, there is a considerable increase in ohmic resistances when the variation of pitches is more than 30%.

V. Comparison of H-Fields by a Circular Loop and an Infinite Straight Wire

Fig. 7(a) and (b) shows the schematic diagrams of a circular loop and an infinite straight wire, respectively. In Fig. 7(a), z- and ρ-directed H-fields H_z and H_ρ are generated by the circular loop of radius r_1. The loop is made of a single filamentary wire. Fig. 7(b) shows the cross-sectional view of the infinite

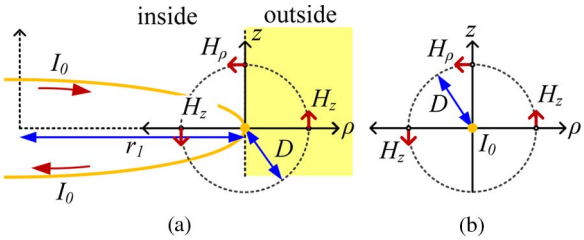

Fig. 7. Schematic diagrams of (a) a circular loop and (b) an infinite straight wire.

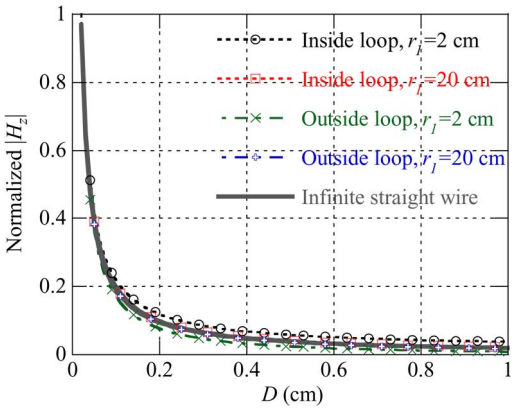

Fig. 8. Calculation results of normalized magnetic fields $|H_z|$ according to D.

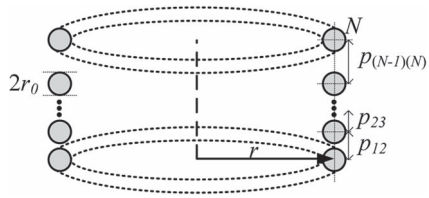

Fig. 9. Schematic diagram of a helical coil.

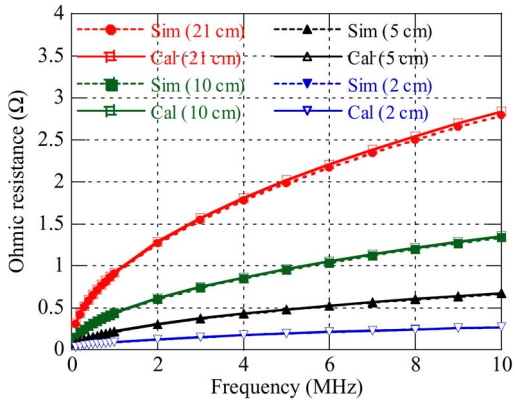

Fig. 10. Comparison of the calculated ohmic resistances and simulation results for helical coils of different radii with equal pitches, when $N = 6$, $r_0 = 0.5$ mm, and $p = 2$ mm.

straight filamentary wire. It is assumed that both centers of the single wire of the circular loop and the infinite straight wire are identical.

Fig. 8 compares calculation results of normalized magnetic fields $|H_z|$ of circular loops of different radii and the infinite straight wire according to the distance (D) from the center of each wire. The H-fields of the circular loop are calculated by referring to [18]. The H-fields of circular loops of small $(r_1 = 2$ cm$)$ and large $(r_1 = 20$ cm$)$ radii are compared to that of the infinite straight wire, respectively. The normalized magnetic fields of the 20-cm circular loop are the same as that of the infinite straight wire according to the distance (D). For the 2-cm circular loop, the results are the same as that of the infinite straight wire at $D < 0.1$ cm where magnetic field is much stronger, and there is a little difference between the results at $D > 0.1$ cm. It is shown that the magnetic field $|H_z|$ of a circular loop is very similar to that of an infinite straight wire. It can be said that the way of calculating ohmic resistance per unit length by using magnetic field by a set of infinite straight wires can be well applied to that for parallel multiloop coils such as spiral coils of round cross section. In addition, it is reported that the calculation method of ohmic resistance for a set of infinite straight wires is applied to that for a circular helical coil [15].

VI. Applications to Helical and Spiral Coils in WPT Systems

In this section, the closed-form formula in (14) is applied to the calculation of circular helical and spiral coils. The conductivity of the copper wire used is 5.8×10^7 in both the calculation and simulation. For the simulation, a commercial electromagnetic FEM simulator (ANSYS Maxwell 2D) is used.

A. Application for Helical Coils With an Equal Pitch

Fig. 9 shows a schematic diagram of a helical coil with arbitrary pitches. r and p_{ij} are the radius of the helical coil and the pitch between the ith and jth loops, respectively. Fig. 10 compares calculated ohmic resistances and simulation results for helical coils with an equal pitch when $N = 6$, $r_0 = 0.5$ mm, and $p = 2$ mm. The total length of the helical coil is $2\pi rN$. The radius of the helical coils, r, is changed from 2 to 21 cm. The results of the calculation are consistent with those of the simulation for the case of a small r of 2 cm, as well as a larger r.

B. Application for Optimization of a Helical Coil With Unequal Pitches

Fig. 11 compares calculated, simulated, and measured ohmic resistances of helical coils with unequal pitches according to r_0 at 6.78 MHz where $N = 6$, $r - r_0 = 45$ mm, $p_{12} = 2.2$ mm, $p_{23} = 2$ mm, $p_{34} = p_{45} = 1.8$ mm, and $p_{56} = 2.2$ mm. The calculated and simulated results are in good agreement. The optimum $r_0 = 0.63$ mm for the minimum ohmic resistance is observed.

Ohmic resistances of fabricated coils are obtained by measuring a quality factor (Q) and self-inductance (L) of the coil, i.e., $R = 2\pi fL/Q$. The resonant frequency (f) of each coil is 6.78 MHz and tuned by using lumped capacitors. The Q-factors of the fabricated helical coils with a solid copper wire of $r_0 =$ 0.3, 0.5, and 0.8 mm are 295.76, 389.52, and 439.87, respectively, and are measured by using a vector network analyzer (Agilent 4395A). Self-inductances of 6.184 μH, 5.992 μH, and 5.671 μH are measured by using an LCR meter, respectively. It shows that the measured ohmic resistances are similar to the calculated and simulated ohmic resistances. The reasons

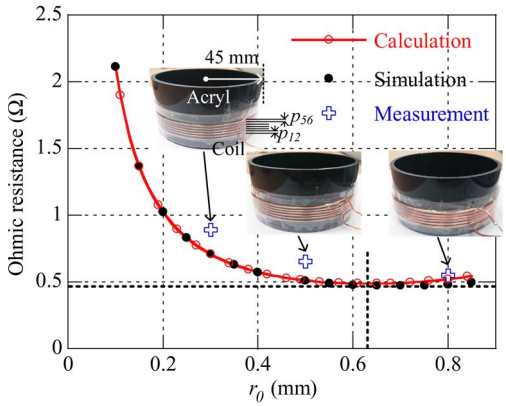

Fig. 11. Comparison of calculated, simulated, and measured ohmic resistances of helical coils with unequal pitches according to r_0 at 6.78 MHz, when $r = 45$ mm, $N = 6$, $p_{12} = 2.2$ mm, $p_{23} = 2$ mm, $p_{34} = p_{45} = 1.8$ mm, and $p_{56} = 2.2$ mm.

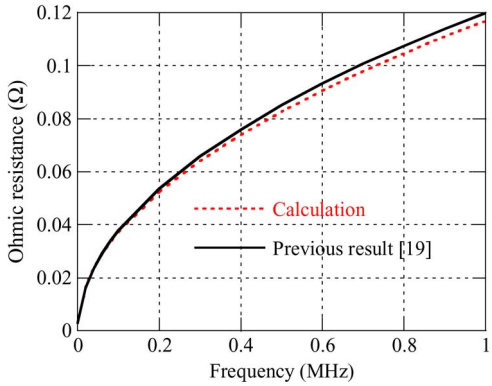

Fig. 12. Comparison of calculated ohmic resistances and results in [19].

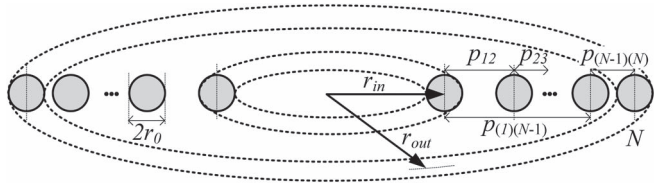

Fig. 13. Schematic diagram of a circular spiral coil.

of the differences are because of the equivalent series resistance (ESR) of lumped capacitors for tuning the resonant frequency and pitch tolerance when the coils of small pitch are made.

C. Application for Spiral Coils With an Equal Pitch

Fig. 12 compares calculated ohmic resistances and results in [19]. The ohmic resistance of a circular spiral coil with an equal pitch has been presented in [19]. A schematic diagram of a spiral coil is displayed in Fig. 13. A tubular copper wire of 3 mm in radius and 1 mm in thickness was used in [19]. In the calculation, the tubular wire is regarded as a solid round wire with a 3-mm radius. The dimensions of the coil were $r_{out} = 14.7$ cm, $r_{in} = 10.3$ cm, $p = 8.8$ mm, and $N = 6$. The total length of the spiral coil is $2\pi[Nr_{in} + \sum_{k=2}^{N-1} p_{(1)(k)}]$. The calculated ohmic resistances of the coil up to 1 MHz were provided. The calculated ohmic resistances have a maximum difference of 5.3% compared to previous values in [19], although a wire in the calculation used in this paper is a solid wire.

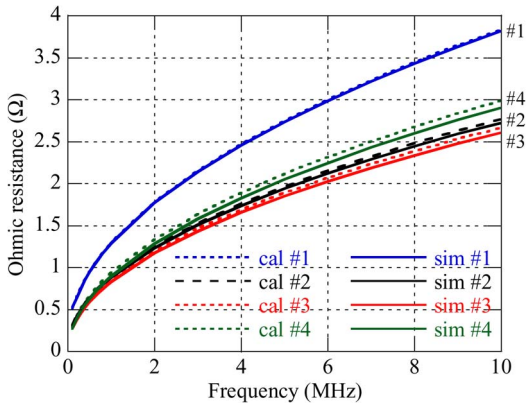

Fig. 14. Comparison of calculated ohmic resistances and simulation results for spiral coils with equal pitches. The minimum resistance was achieved in #3.

D. Application for Optimization of a Spiral Coil With an Equal Pitch

For efficient WPT, a lower ohmic resistance of the coil is very important. The results of (14) and (15) can be also applied to designing a spiral coil of the lowest ohmic resistance with an equal pitch when a winding width W and the number of turns, N, are fixed.

Fig. 14 shows the calculated ohmic resistance and the simulation for spiral coils with an equal pitch. The $r_{in} - r_0$ and $r_{out} + r_0$ are 199.5 and 210.5 mm, respectively. In the coil, $W(= r_{out} - r_{in} + d)$ is fixed at 11 mm. $N = 6$ is determined. For comparison, four cases are considered as follows:

$$\begin{aligned}
&\#1 : r_0 = 0.3 \text{ mm},\ p = 2.08 \text{ mm};\\
&\#2 : r_0 = 0.5 \text{ mm},\ p = 2 \text{ mm};\\
&\#3 : r_0 = 0.6 \text{ mm},\ p = 1.96 \text{ mm};\\
&\#4 : r_0 = 0.8 \text{ mm},\ p = 1.88 \text{ mm}.
\end{aligned}$$

In case #3, the OMR was calculated using (15) for the coil. Dotted and solid lines represent calculation and simulation results, respectively. The results show that the lowest ohmic resistance is obtained in #3. The calculation and simulation results agree. It can be found that the resistance by skin effects is dominant in case #1 up to 10 MHz since p/d is large. Resistance in #4 is higher than that in #3, although the radius in #4 is larger than that in #3, particularly at higher frequencies. The reason is that the proximity effect for #4 is higher than that for #3. Furthermore, the results also verify that the minimum ohmic resistance can be obtained using (15). Therefore, optimized low-loss coils can be designed easily using the OMR formula for spiral coils with an equal pitch.

E. Application for Optimization of a Spiral Coil With Unequal Pitches

One useful application of a spiral coil with unequal pitches is for free-positioning WPT because spiral coils with unequal pitches, which are finely designed, have the advantage of uniform H-field distribution [10], [11]. Therefore, by determining

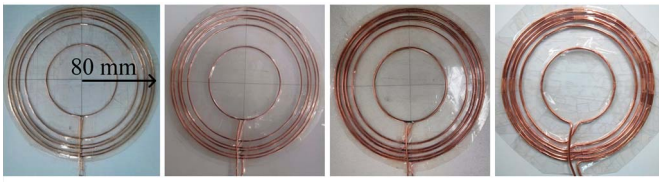

Fig. 15. Fabricated spiral coils with the unequal pitches: (a) $r_0 = 0.3$ mm, (b) $r_0 = 0.5$ mm, (c) $r_0 = 0.8$ mm, and (d) $r_0 = 1.3$ mm.

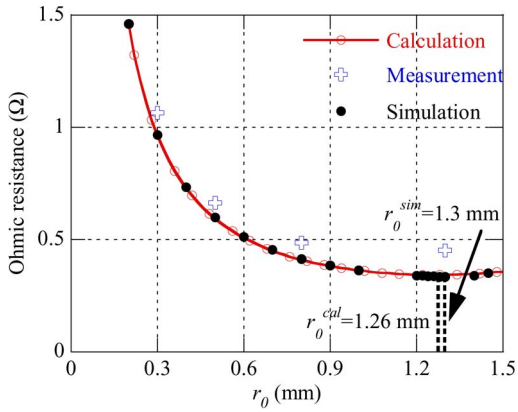

Fig. 16. Comparison of calculation, simulation, and measurement results of the ohmic resistances for Tx spiral coils with unequal pitches.

an optimum wire radius, it is possible to minimize the ohmic resistance of the coils with unequal pitches.

It is assumed that an Rx coil is a circular spiral coil with an equal pitch ($N = 5$, $r_{out} = 23.5$ mm, and $p = 1$ mm) for the application of charging mobile devices. For uniform H-fields, a circular spiral Tx coil with unequal pitches is designed by using the Neumann formula for mutual inductance between two circular loops [20]. A target distance (g) between the Tx and Rx coils is set to 10 mm. The operating frequency is 6.78 MHz. As a result, the Tx coil is designed as $r_{out} = 80$ mm, $r_{in} = 39$ mm, $N = 6$, $p_{12} = 23$ mm, $p_{23} = 7$ mm, $p_{34} = 3$ mm, $p_{45} = 5$ mm, and $p_{56} = 3$ mm. The calculation of the mutual inductances of the coils is conducted via a filament method. The wire radius does not considerably affect the results in general. The calculated mutual inductance is about 437 nH when the radial displacement of the Rx coil is within 45 mm.

Fig. 15(a)–(d) shows the fabricated Tx coils made of solid copper wires with radii of 0.3, 0.5, 0.8, and 1.3 mm, respectively. The measured Q-factors of each coil are 302.39, 469.16, 612.96, and 624.84, respectively. The measured self-inductances are 7.560, 7.299, 7.007, and 6.635 μH, respectively. From the Q-factors and self-inductances of the coils, the measured ohmic resistances are obtained at the frequency ($f = 6.78$ MHz).

Fig. 16 shows the comparison of calculation, simulation, and measurement results of ohmic resistances for the Tx coils. The calculated ohmic resistances of the coils, according to r_0, are consistent with the simulation results. The measured results are also in agreement with the calculated and simulated results. The differences between measurement and calculation are 0.1 Ω at $r_0 = 0.8$ mm and 0.12 Ω at $r_0 = 1.3$ mm, respectively. The reason is that the ESR of lumped capacitors is added. Also, small error in measuring high Q-factor for $r_0 = 1.3$ mm is included.

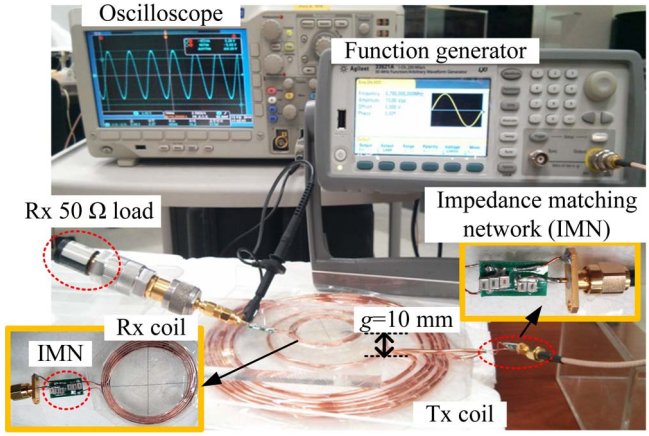

Fig. 17. Measurement setup for the WPT system with the optimum Tx and Rx coils.

From Fig. 16, the optimum radius for minimum ohmic resistance can be also obtained. The calculated optimal ohmic resistance of the Tx coil is 343.2 mΩ at $r_0 = 1.26$ mm, while the simulated optimum resistance is 335.47 mΩ at $r_0 = 1.30$ mm. The calculated and simulated optimum radii are well consistent.

F. Experiment of a WPT System

Fig. 17 shows the measurement setup for a WPT system using two coils. For the system, the optimized Tx coil in Fig. 15(d) is used. The optimum formula of (15) is used to design an optimal Rx coil for the case of $N = 5$, $r_{out} = 23.5$ mm, $p = 1$ mm, and $W = (N-1)p + 2r_0$ as explained in Section IV-B and referring to Fig. 5. The optimum radius of the Rx coil, $r_0 = 0.35$ mm, is obtained. Considering the standard wire gauge, an Rx spiral coil with $r_0 = 0.3$ mm is fabricated as the optimized Rx coil. The calculated ohmic resistance of the Rx coil is 384.8 mΩ. The measured ohmic resistance of the Rx coil is 418 mΩ where the measured Q-factor and self-inductance are 203.33 and 1.993 μH, respectively. The measured ohmic resistance of the Rx coil is consistent with the calculation.

Regarding the influence of a parallel multiloop Rx coil on the ohmic resistance of a parallel multiloop Tx coil, it can be said that the ohmic resistance may be changed by the proximity effect between Tx and Rx coils when Tx and Rx coils are very similar and placed concentrically and the ratio of the distance of two neighboring loops and the wire diameter of the coils is close to 1. From the viewpoint of practical applications, Tx and Rx coils are different in size and somewhat apart. Therefore, the proximity effect between Tx and Rx coils can be negligible, and the proposed calculation and optimization methods are still valid.

An input power of 250 mW at 6.78 MHz is supplied to the Tx coil by using a function generator (Agilent 33521A). A receiving power of 234.26 mW at an Rx load of 50 Ω is measured by using an oscilloscope (Tektronix DPO3032). Capacitive impedance matching networks shown in [2] are used for satisfying optimum impedance matching conditions [1]. As a result, the measured power transfer efficiency of

the WPT system with the optimized Tx coil is 93.7% at the center and 93.2% at 40 mm in the radial displacement due to the uniform H-field distribution of the Tx coil, respectively, when the distance $g = 10$ mm. The measured power transfer efficiency with the Tx coil shown in Fig. 15(a) is 90.2% at the center and 90.1% at 40 mm when the distance $g = 10$ mm. In addition, power transfer efficiencies of 34.67% are obtained at the center by using the optimized Tx coil for $g = 150$ mm. On the other hand, an efficiency of 14.16% is achieved by using the Tx coil shown in Fig. 15(a) for $g = 150$ mm. That is, power transfer efficiency by using the optimized Tx coil is enhanced by 20%. Therefore, the results show that the coil of lower ohmic resistance has higher power transfer efficiency, particularly as the mutual inductance between Tx and Rx coils decreases.

VII. Conclusion

A simple approximate closed-form formula to calculate ohmic resistance in a system of parallel round conductor wires with equal and unequal pitches is proposed. A detailed derivation procedure and some useful calculation results are also provided. It is shown that the formula can be well applied to multiloop coils (e.g., spiral and helical coils) with both equal and unequal pitches. It is verified that the calculation results are consistent with the simulation results, the previous results, and the measured results for the practical helical and spiral coils. It is shown that, by using the formula, the ohmic resistance of spiral coils with equal and unequal pitches can also be minimized for a highly efficient system of magnetic resonance WPT. Therefore, it is expected that the derived formula and method can be effectively applied to calculate the resistance and optimize various multiloop conductor coils for highly efficient WPT.

Acknowledgment

The authors would like to thank Prof. H. J. Eom from the KAIST, Korea, for his valuable comments.

References

[1] A. Kurs *et al.*, "Wireless power transfer via strongly coupled magnetic resonances," *Science*, vol. 317, no. 5834, pp. 83–86, Jul. 2007.
[2] L. Chen, S. Liu, Y. C. Zhou, and T. J. Cui, "An optimizable circuit structure for high-efficiency wireless power transfer," *IEEE Trans. Ind. Electron.*, vol. 60, no. 1, pp. 339–349, Jan. 2013.
[3] R. Johari, J. V. Krogmeire, and D. J. Love, "Analysis and practical considerations in implementing multiple transmitters for wireless power transfer via coupled magnetic resonance," *IEEE Trans. Ind. Electron.*, vol. 61, no. 4, pp. 1774–1783, Apr. 2013.
[4] R. Johari, J. V. Krogmeier, and D. J. Love, "Analysis and practical considerations in implementing multiple transmitters for wireless power transfer via coupled magnetic resonance," *IEEE Trans. Ind. Electron.*, vol. 61, no. 4, pp. 1774–1783, Apr. 2014.
[5] W. Zhong, C. K. Lee, and S. Y. R. Hui, "General analysis on the use of Tesla's resonators in domino forms for wireless power transfer," *IEEE Trans. Ind. Electron.*, vol. 60, no. 1, pp. 261–270, Jan. 2013.
[6] A. P. Sample, D. T. Meyer, and J. R. Smith, "Analysis, experimental results, range adaptation of magnetically coupled resonators for wireless power transfer," *IEEE Trans. Ind. Electron.*, vol. 58, no. 2, pp. 544–554, Feb. 2011.
[7] M. Yang, G. Yang, E. Li, Z. Liang, and H. Lin, "Modeling and analysis of wireless power transmission system for inspection robot," in *Proc. IEEE ISIE*, 2013, pp. 1–5.
[8] T. C. Beh, M. Kato, T. Imura, S. Oh, and Y. Hori, "Automated impedance matching system for robust wireless power transfer via magnetic resonance coupling," *IEEE Trans. Ind. Electron.*, vol. 60, no. 9, pp. 3689–3698, Sep. 2013.
[9] J. Wang *et al.*, "Lateral and angular misalignments analysis of a new PCB circular spiral resonant wireless charger," *IEEE Trans. Magn.*, vol. 48, no. 11, pp. 4522–4525, Nov. 2012.
[10] E. Waffenschmidt, "Free positioning for inductive wireless power system," in *Proc. IEEE ECCE*, 2011, pp. 3480–3487.
[11] J. J. Casanova, Z. N. Low, J. Lin, and R. Tseng, "Transmitting coil achieving uniform magnetic field distribution for planar wireless power transfer system," in *Proc. IEEE RWS*, 2009, pp. 530–533.
[12] A. H. M. Arnold, "Proximity effects in solid and hollow round conductors," *J. Inst. Elect. Eng. II, Power Eng.*, vol. 88, no. 4, pp. 349–359, Aug. 1941.
[13] X. Nan and C. R. Sullivan, "Simplified high-accuracy calculation of eddy-current losses in round-wire windings," in *Proc. IEEE PESC*, 2004, pp. 873–879.
[14] J. A. Ferriera, "Improved analytical modeling of conductive losses in magnetic components," *IEEE Trans. Power Electron.*, vol. 9, no. 1, pp. 70–79, Jan. 1994.
[15] G. Smith, "The Proximity Effect in Systems of Parallel Conductors and Electrically Small Multiturn Loop Antennas," Div. Eng. Appl. Phys., Harvard Univ., Cambridge, MA, USA, Tech. Rep. No. 624, 1971.
[16] C. D. Sijoy and S. Chaturvedi, "Calculation of accurate resistance and inductance for complex magnetic coils using the finite-difference time-domain technique for electromagnetics," *IEEE Trans. Plasma Sci.*, vol. 36, no. 1, pp. 70–79, Feb. 2008.
[17] J. Lammeraner and M. Stafl, *Eddy Currents*. London, U.K.: Iliffe Books, 1966.
[18] R. H. Good, "Elliptic integrals, the forgotten functions," *Eur. J. Phys.*, vol. 22, no. 2, pp. 119–126, Mar. 2001.
[19] Z. Pantic, B. Heacock, and S. Lukic, "Magnetic link optimization for wireless power applications: Modeling and experimental validation for resonant tubular coils," in *Proc. IEEE ECCE*, 2012, pp. 3825–3832.
[20] D. K. Cheng *Field and Wave Electromagnetics*, 2nd ed. Reading, MA, USA: Addison-Wesley, 1989.

Jinwook Kim (S'11–M'14) received the B.S. degree in electronic engineering from Ajou University, Suwon, Korea, in 2009 and the Ph.D. degree in power electrical equipment information and communications engineering from the University of Science and Technology (UST), Ansan, Korea, in 2014.

Since September 2014, he has been with the Korea Electrotechnology Research Institute, Ansan, as a Postdoctoral Researcher. His research interests include electromagnetic theory and wireless power transfer.

Dr. Kim was the recipient of the Best Paper Award at the 2011 IEEE International Microwave Workshop Series on Innovative Wireless Power Transmission (IMWS-IWPT) from the IEEE Microwave Theory and Techniques Society (MTT-S).

Young-Jin Park (M'03) received the B.S. degree from Chung-Ang University, Seoul, Korea, in 1997, the M.S. degree in electrical engineering from the KAIST, Taejon, Korea, in 1999, and the Dr.-Ing. degree in electrical engineering and information technology from the Karlsruhe Institute of Technology (KIT), Karlsruhe, Germany, in 2002.

From March 2002 to October 2002, he was a Research Associate at the Institut fuer Hochfrequenztechnik und Elektronik (IHE), KIT. In November 2002, he joined the Korea Electrotechnology Research Institute, Ansan, Korea, where he is currently a Principal Researcher. Since March 2005, he has been an Adjunct Professor at the University of Science and Technology, Ansan. His research interests include high resolution impulse radio based-UWB sensors (UWB RTLS, GPR, and TDR), wireless power transfer based on magnetic resonance and microwave, and millimeter-wave antennas and propagation for automotive radar.